PHYSICAL REVIEW B

CONDENSED MATTER

THIRD SERIES, VOLUME 54, NUMBER 5 1 AUGUST 1996-I

BRIEF REPORTS

Brief Reports are accounts of completed research which, while meeting the usual **Physical Review B** *standards of scientific quality, do not warrant regular articles. A Brief Report may be no longer than four printed pages and must be accompanied by an abstract. The same publication schedule as for regular articles is followed, and page proofs are sent to authors.*

Numerical study of excitons in a two-dimensional organic dye aggregate

Akihiro Tomioka and Kenjiro Miyano

Department of Applied Physics, Faculty of Engineering, University of Tokyo, Hongo 7-3-1, Bunkyo-ku, Tokyo 113, Japan

(Received 1 December 1995; revised manuscript received 19 March 1996)

A simple numerical simulation taking into account the on-site energy disorder within a two-dimensional (2D) dye aggregate has been successfully employed to reproduce both the absorption and fluorescence spectra observed experimentally in organic dye monolayers. The amount of the on-site energy disorder required for the fit was found to be quite large (90% of the excitation transfer energy) even at low temperature and yet the excitons spread over >100 molecules spatially, which is a good manifestation of the 2D nature of the excitons. Detailed investigation of the relaxation process prior to the fluorescent emission revealed that relaxation is so dominant that even if higher energy levels in the exciton band are excited, they should relax down with a probability ~ 1 to the lowest 0.4% levels at the exciton band bottom before they fluoresce and only with less than 10 relaxation steps. This was found to be due to high extent of wave function overlap between the exciton levels, and it accounts for a short but finite time lag between the excitation at the band top and the fluorescence decay. [S0163-1829(96)07529-7]

I. INTRODUCTION

Strong interaction between organic dye molecules in aggregate makes excitons a suitable description of their excited eigenstates.[1] One-dimensional (1D) exciton states in dye aggregates have been studied extensively. The theoretical analysis based on a model Hamiltonian has been shown adequate to describe the experimental observation[2] except for the details, such as the ''correlated disorder.''[3] However, not much attention has been paid to the effect of the dimensionality on the exciton states in dye aggregates. Since the excitation can extend easily in higher dimensions, the delocalization parameter (number of molecules within the coherence length of an exciton) should be larger in a two-dimensional (2D) system than in a 1D system.

Recently we have demonstrated a 2D nature of the excitons in a monolayer of a cyanine dye.[4] Here we present the results of a simple numerical study to elucidate the nature of excitons in two-dimensional organic dye aggregates. It should be stressed that not only the absorption spectrum but also the fluorescence spectrum and other optical properties observed experimentally can all be reproduced from a single model.

II. NUMERICAL MODEL

After the seminal numerical study of excitons by Schreiber and Toyozawa,[5] various degrees of sophistication have been tried. The off-diagonal disorder have been taken into account with the long-range dipole-dipole interaction.[2,6] The correlated diagonal disorder has been also considered in order to explain the anomalous nonlinear behavior.[3]

For the current study of 2D excitons, however, we restrict ourselves to the simplest case of the Gaussian diagonal disorder and the nearest neighbor interaction without disorder. The reason is partly because of the computational difficulty in treating much larger matrices in a 2D system. But it is mostly because the simple model can reproduce the experimental results reasonably well, as will be shown below.

Thus, our model Hamiltonian is the following:

$$\boldsymbol{H}=\sum_i \epsilon_i a_i^\dagger a_i+\sum_{\text{nearest}}\sum_{\text{neighbor}(i,j)} V a_i^\dagger a_j, \qquad (1)$$

where the operator $a_i^\dagger$ (a_i) excites (deexcites) the ith molecule (with the excitation energy ϵ_i). V is the transfer energy of the excitation from the jth molecule to the ith molecule

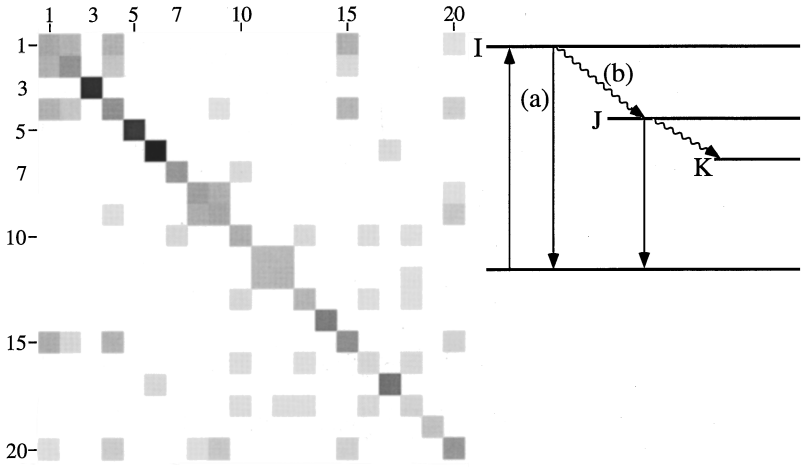

FIG. 1. Gray scale map of the extent of wave function overlap between the Ith exciton (ordinate) and the Jth exciton (abscissa). The diagonal element is equivalent to the inverse magnitude of delocalization parameter of the corresponding exciton. Inset: Model of deexcitation. After being photoexcited, state I either (a) emits a photon or (b) relaxes to another state J of lower energy with a branching ratio R.

and is included only for the nearest neighbors. The on-site energy has a Gaussian disorder with the standard deviation D.

The Hamiltonian [Eq. (1)] has been diagonalized with a fixed V (deduced from the experiment) and a varying parameter $D/|V|$ (degree of disorder). The cyclic boundary condition was not employed to see the size effect.

III. RESULTS AND DISCUSSIONS

A. Relaxation process

In our previous study,[4] it was shown that the absorption spectrum can be well reproduced by choosing $D/|V|=0.9$, where $|V|$ was found experimentally to be 514 cm^{-1} and the average of on-site energy was 19440 cm^{-1}. The fluorescence spectrum was reproduced if we assumed that the lowest six exciton levels fluoresce (only 0.4% of the number of total exciton levels). This fact reveals the strong tendency of relaxation from the initial excited state far down to the lowest localized states. Although the overall profile was in good agreement, there was an abrupt drop in the high energy side of the simulated spectrum due to the artificial restriction of the fluorescent sites.

To get more realistic spectrum we must take into consideration the probability of fluorescence from a given state, tracing the relaxation process from the initial excited state down to the final fluorescing state. Then we can construct the fluorescence spectrum by making a histogram of this final fluorescence process weighed with the calculated probability. We assume that the relaxation between exciton states is mediated by the linear exciton-phonon coupling, $\Sigma_i g a_i^\dagger a_i (b_i^\dagger + b_i)$, where $b_i^\dagger + b_i$ is the molecular deformation operator and we assume that the exciton couples effectively to the intramolecular vibrations that have large density of states spread over the energy scale of our interest (<500 cm^{-1}). This interaction is already folded into the disorder parameter D together with the static disorder and therefore, within the time scale in which the Frank-Condon principle applies, no interaction between exciton states should exist. However, since the lifetime of an exciton is expected to be much longer than the period of relevant vibrations, the exciton created is no longer an eigenstate at a later time. A simple argument can be made[4] to show that the transition between exciton states are proportional to the wave function overlap defined as

$$W(I,J)=\sum_{i=1}^{M} u_{Ii}^2 u_{Ji}^2, \tag{2}$$

where u_{Ii} is the amplitude of the Ith exciton wave function at the ith molecule.

Figure 1 shows the value of Eq. (2) in gray scale obtained in a single calculation on a system composed of $M=1444(38\times 38)$ molecules. The diagonal elements represent the degree of localization[7] whereas the off-diagonal elements show the transition probability between the two states. Starting from any exciton state, one can easily trace all possible relaxation pathways on this map. If we take a higher exciton level as the initial excited state, the number of relaxation pathways grows rapidly, which forces us to treat the relaxation process statistically.

B. Fluorescence simulation based on a relaxation model

Based on the argument of the previous section, we propose a model for fluorescence simulation taking into account the relaxation path network. Inset in Fig. 1 depicts the basic notion of the model. Upon absorbing a photon, the system is excited up to one of the exciton levels I with the probability proportional to the transition moment squared. Then the system (a) emits a photon or (b) relaxes to another exciton state J with a branching probability proportional to the ratio of the transition moment squared (fluorescence, f) to the wave function overlap between I and J states (relaxation, r), which can be expressed as

$$\frac{P_f(I)}{P_r(I,J)}=R\frac{|M(I)|^2}{W(I,J)}, \tag{3}$$

using a scaling factor R. Here we completely neglected the nonradiative transition to the ground state, which can be justified by the high quantum efficiency of the fluorescence from a 2D dye aggregate at low temperature.[8]

Employing this relaxation-emission branching model, fluorescent emission spectrum was calculated by varying the scaling factor R. To reduce the computational load, the aggregate size was reduced to 28×28 and the spectrum was deduced from 200 calculations. The resulting spectrum is

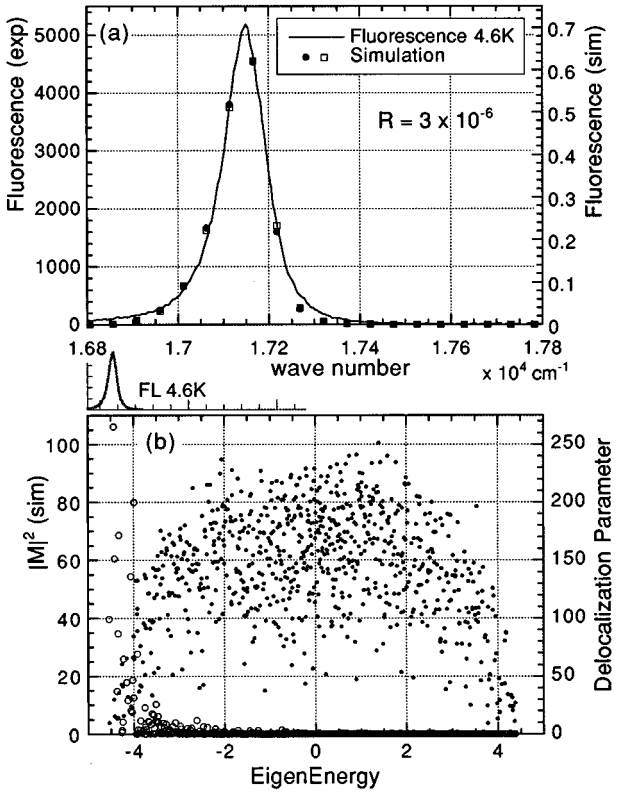

FIG. 2. (a) Fluorescence spectrum of the aggregate. Note the good fit on both sides of the peak between the experimental spectrum (solid line) at 4.6 K and the simulation (shown by dots) based on the relaxation model with $R=3\times10^{-6}$. Both were performed with a photoexcitation at $2.04-2.22\times10^4$ cm^{-1}. Identical spectrum results when the simulation is performed with the whole exciton band photoexcited uniformly (shown by squares). (b) Distribution of the transition moment (shown by open circles) and the delocalization parameter (dots) of exciton over the whole eigenenergy region obtained from a single calculation.

shown with dots in Fig. 2(a). Here, the system is photoexcited uniformly by illuminating over 450 to 490 nm, which corresponds to the experimental condition. Since the energy scaling specified by the transfer energy V was determined by the fitting to absorption spectrum, R was the only parameter to vary. When we increased R, fluorescence process became preferred to the relaxation process [Eq. (3)], and therefore the spectrum peak shifted to higher energy making the peak width broader. When we set $R=3\times10^{-6}$, the fluorescence spectrum best fits to the experimental data as shown in Fig. 2(a). The good agreement both on the low energy side and the high energy side of the peak is now clear, which is an improvement over the previous model.[4] At the liquid He temperature phonon is not expected to scatter excitons to higher energy, which justifies the current model that treats relaxation process only to lower energy levels.

The fluorescence spectrum was essentially the same for $R\leqslant10^{-6}$. This implies that in the real aggregates the relaxation proceeds all the way down to the states which are ''trapped'' in the sense that no further relaxation to lower states is possible due to the lack of wave function overlap (e.g., levels 3, 5, 6, and 7 in Fig. 1). Hence these states are spatially isolated. Figure 2(b) shows that (a) the transition moment is large and (b) the delocalization parameter

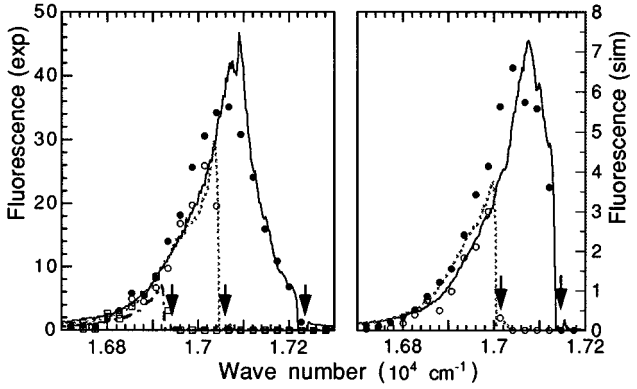

FIG. 3. Measured fluorescence spectra (lines) under photoexcitation within the fluorescence band (indicated by arrows) and the results of simulation (dots) corresponding to the respective experimental conditions.

$(1/\Sigma_{i=1}^{M}|u_{Ii}|^4)$ is small for the exciton states at the band bottom whereas the reverse holds for the remaining exciton states. Therefore, relaxation is very efficient for the large majority of exciton levels independent of the magnitude of R as far as it is small enough, effectively funneling all energy down to the ''trapped'' states.

C. Fluorescence with selective excitation

From the discussions in the previous section, it is expected that the fluorescence spectrum is rather insensitive to the excitation photon energy. This has been confirmed experimentally and can be reproduced numerically as follows.

The simulation shown with dots in Fig. 2(a) has been performed with a photoexcitation between 450 and 490 nm, which is at the top of the exciton band. An identical fluorescence spectrum resulted as shown with squares in the same figure, when calculation was performed assuming that the entire exciton band (450–600 nm) has been uniformly excited.

Average number of relaxation steps from a given starting exciton has been found to be very small. Less than ten relaxation steps are needed to travel even top-to-bottom of the exciton band. The number was found to be effectively independent of the aggregate size: 7.1 ± 0.3, 7.3 ± 0.3, and 7.4 ± 0.3 for $M=784$, 1444, and 2304, respectively, under the same photoexcitation over 450 nm through 490 nm. A preliminary fluorescence lifetime measurement at 80 K shows that the decay rate is ~10 ps reflecting the large oscillator strength of the fluorescing states. The decay occurred immediately after the resonant excitation but a dwell time of ~25 ps was observed when excited at 380 nm. This observation is in line with our relaxation model.

Based on the same argument as above, we expect no quantitative difference in the fluorescence spectrum when excited within fluorescence band. Figure 3 shows the result of experiments using a cw dye laser with a linewidth of 15 cm^{-1}. Note that the fluorescence profiles are essentially the same below the excitation energy (indicated by arrows). In Fig. 3, we also plotted the results of fluorescence simulations based on the relaxation model. The essential features of the spectra are reproduced. For this specimen the absorption spectrum was fitted with $D/|V|=1.0$ and $|V|=534$ cm^{-1} and a scaling factor $R=7\times10^{-5}$ was used to reproduce the fluorescence spectra. The exact value of R is unimportant as

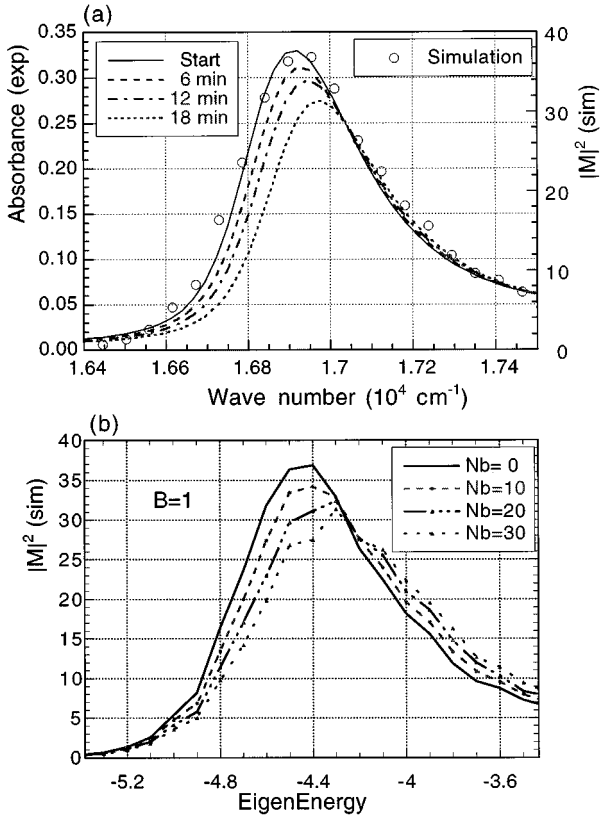

FIG. 4. Absorbance change induced by photobleaching. (a) Successive absorption spectra recorded at room temperature in every 6 min while the specimen was illuminated continuously with a room light. (b) Simulated absorption spectrum, the original and those after ''photobleaching'' 10, 20, and 30 molecules. Since the experiment was performed at room temperature, the best-fit disorder parameter was $D/|V|=1.1$.

discussed in Sec. III B. Although the actual peaks appear sharper than those reproduced by the simulation, the spikes 120 cm^{-1} below the excitation energy is the Raman band; after removing their contribution the peak shape matches the simulation. The excitation beam linewidth was set twice as wide in the simulation as the actual linewidth to reduce the iteration number of calculation. Even under this condition, 2000 iterations of calculation were necessary to produce the spectrum because chances were few to have absorbing exciton levels falling within the excitation linewidth.

D. Photobleaching

The photobleaching occurs in a very distinct manner as shown in Fig. 4(a). While the low energy edge of the spectrum is bleached, the shoulder at the high energy side does not change appreciably.

Because the photobleaching is likely to be due to the oxidation of the double bond in the dye molecule and subsequent loss of the absorption energy level in the visible, we model the process by setting the on-site energy of the ''bleached'' molecule to be $+2D$ and by removing all the excitation transfer to that molecule. This effectively eliminates the molecule from contributing to the optical absorption. The molecules to be bleached were selected as those having the largest wave function amplitude of an exciton level. The candidate exciton level was selected statistically with a probability proportional to the resident time during which the excitation is expected to stay in that level in the relaxation/fluorescence process. This excitation resident time should be inversely proportional to the decay rate, i.e., the sum of (1) the fluorescing rate of the level and (2) the relaxation rate away from that level. Hence, using a scaling factor B, we took the bleaching probability of a level I as

$$P_{\mathrm{bl}}(I)=\frac{B}{R|M(I)|^2+\Sigma_{J=1}^{I-1}W(I,J)}, \tag{4}$$

which is consistent with Eq. (3). In this model, an excitation at a level I can take three paths: (1) fluorescence, (2) relaxation, and (3) bleaching. Adding the third branch to the previous fluorescence model in Sec. III B, bleaching probability of each exciton level was calculated.

The actual calculation was performed as follows. An exciton level was picked up according to the bleaching probability. Five molecules with the largest amplitudes in this level were ''bleached'' at once, and then the whole exciton levels were recalculated. This bleaching and recalculation was repeated six times. The resulting absorption spectrum is shown in Fig. 4(b): the initial one and those after bleaching total of 10, 20, and 30 molecules. Basic feature of the change is well reproduced, diminishing only at the low energy side and leaving high energy shoulder not very much affected. Note that, although only the low energy edge is bleached, it does not mean that the molecules responsible for these low-lying levels are bleached as was originally inferred in Ref. 4. In fact, if only these molecules are bleached, the net result is a significant *increase* in the absorption near the absorption peak.

In the strict sense of the model, only one molecule should be bleached at a time from one exciton level. We chose to bleach five molecules instead to save computation time. A similar calculation in which only one molecule was bleached at a time but with a smaller aggregate size (20×20) showed a similar result.

IV. CONCLUSION

The absorption and the fluorescence spectrum observed in a two-dimensional cyanine dye aggregate have been successfully reproduced by a numerical simulation with the same set of parameters taking into account the on-site energy disorder. The ''trapped'' states, which have been identified at the exciton band bottom as having large transition moment and as showing localized spatial distribution, have proven to be solely responsible for the fluorescence. This was further supported by the characteristic photobleaching showing good agreement between experiment and simulation. The remaining majority of the excited states, with small transition moment and being less localized in the aggregate, have been found to highly overlap among one another and therefore produce a fast and near-perfect relaxation down to the lowest ''trapped'' states.

ACKNOWLEDGMENTS

We are indebted to Akira Nabetani who kindly let us use the experimental data. This work was supported in part by a Grant-in-Aid for Scientific Research from the Ministry of Education, Science, and Culture, partly by The Kurata Research Grant, and by a grant from Takeda Science Foundation.

[1] A.S. Davydov, *Theory of Molecular Excitons* (Plenum, New York, 1971).

[2] J. Moll, S. Daehne, J.R. Durrant, and D.A. Wiersma, J. Chem. Phys. **102**, 6362 (1995); H. Fidder and D.A. Wiersma, Phys. Rev. Lett. **66**, 1501 (1991); H. Fidder, J. Knoester, and D.A. Wiersma, J. Chem. Phys. **95**, 7880 (1991), and references therein.

[3] J. Knoester, Jpn. J. Appl. Phys. Suppl. **34**, 275 (1995); F. Dominguez-Adame, Phys. Rev. B **51**, 12 801 (1995).

[4] A. Nabetani, A. Tomioka, H. Tamaru, and K. Miyano, J. Chem. Phys. **102**, 5109 (1995).

[5] M. Schreiber and Y. Toyozawa, J. Phys. Soc. Jpn. **51**, 1528 (1982); **51**, 1537 (1982); **51**, 1544 (1982).

[6] A. Malyshev and P. Moreno, Phys. Rev. B **51**, 14 587 (1995).

[7] D.J. Thouless, Phys. Rep. **13**, 93 (1974).

[8] H. Gruhl, H.P. Dorn, and K. Winzer, Appl. Phys. B **38**, 199 (1985).